3. SEISMIC SITE AMPLIFICATION

3.1 Introduction

The Earthquake-resistant design of new structures and their evaluation should take into account their response to site ground motions. And as has been mentioned above, it is clear that the local geology in some areas in Rawabi, where there are soft sediments of marl, clay marl and chalky limestone, will be potential areas of seismic amplification. Areas of seismic amplification occur where the soil and rock at a site have specific characteristics that can significantly amplify the incoming earthquake motion as it travels from earthquake sources.

Recent studies of large destructive earthquakes have shown that damage during the earthquakes is often caused by the amplification of seismic waves in near-surface geology [15-20]. In these cases the post disaster damage assessment shows that the local site effect may make a dominant contribution to the intensity of damage and destruction.

The estimation of site response is therefore critical, in order to evaluate the seismic hazard potential of a given area. Since sedimentary deposits are often the prime locations for development of urban areas, local amplification is a major concern in earthquake-prone regions. It is also a major concern in moderate seismicity areas where developed mid-size cities may struggle with future destructive events due to the combination of site effects and urban development. In the present study, the local site effect on ground-motion amplification and buildings were studied in Rawabi City, stage 1 – phase 1 (see Fig. 1.4 or appendix 1.2).

3.2 Methodology and Data Analysis

3.2.1 Nakamura's Technique

One of the most appealing techniques for estimating site response is Nakamura's method [25] since it only requires records from a single three-component station deployed at the site of interest and does not need a reference seismogram measured at the substratum bedrock. As introduced by Nakamura [25], the technique was intended to assess S-wave amplification from microtremor measurements. There are four components of spectral amplitudes involved in this one-layer problem, namely, the horizontal components of motion at the surface and bottom of the sedimentary layer, referred to as $H_s(f)$ and $H_b(f)$, respectively; and the vertical components of motion at surface and bottom, correspondingly denoted as $V_s(f)$ and $V_b(f)$.

The prime objective of Nakamura's technique is to isolate the amplification effect suffered by horizontal components of substratum motion. In order to do this, he first constructs the theoretical borehole ratios that are widely regarded as the most reliable transfer function estimates for horizontal and vertical components, as given below, respectively:

$$S_h = \frac{H_s}{H_b} and \qquad (1)$$

$$S_v = \frac{V_s}{V_b} \qquad (2)$$

With these two ratios Nakamura constructs an additional transfer function S_t which gives formally the factor by which the horizontal ratio exceeds the vertical one:

$$S_t = \frac{S_h}{S_v} = \frac{H_s / H_b}{V_s / V_b} or \qquad (3)$$

$$S_t = \frac{H_x / V_s}{H_b / V_b} \qquad (4)$$

3.2.2 Microtremor Measurements

Several points have been selected in different sites of Rawabi city (see Fig. 3.1). The criteria for each point are the variations in the geology as well as in the topography. Some points have been measured on rock cover of mainly limestone, chalk and marl (mountain areas) among other points selected to be on soil. Microtremor measurements were carried out at 12 selected sites to account for different geological formations and to cover a comprehensive area in order to give a macrozonation general idea about the dominant frequency in the study area, see Fig 3.1.

The site effects have been investigated by taking measurements of ambient noise collected by short period seismic stations and making the spectral analysis using the following package programs: SDA software for data acquisition and SEISPECT for data analysis (see appendix no. 3). The measurements were made during the daytime (see photos – appendix 3.3), when the contaminating effects of traffic and industrial noise were significant.

Figure 3.1: Locations of selected sites for microtremor measurements

3.2.3 Spectral Analysis Results

The analysis of ambient vibration measurements developed a spectral ratio site response for each site. An example of average Fourier spectra for selected windows and the relation between dominant frequency at the site and the amplification factor (spectral ratio) is presented in Figures. 3.2 – 3.13 for the selected sites shown in Fig. 3.1. The dominant frequency (or period) and its amplification factor of all measured locations are presented in

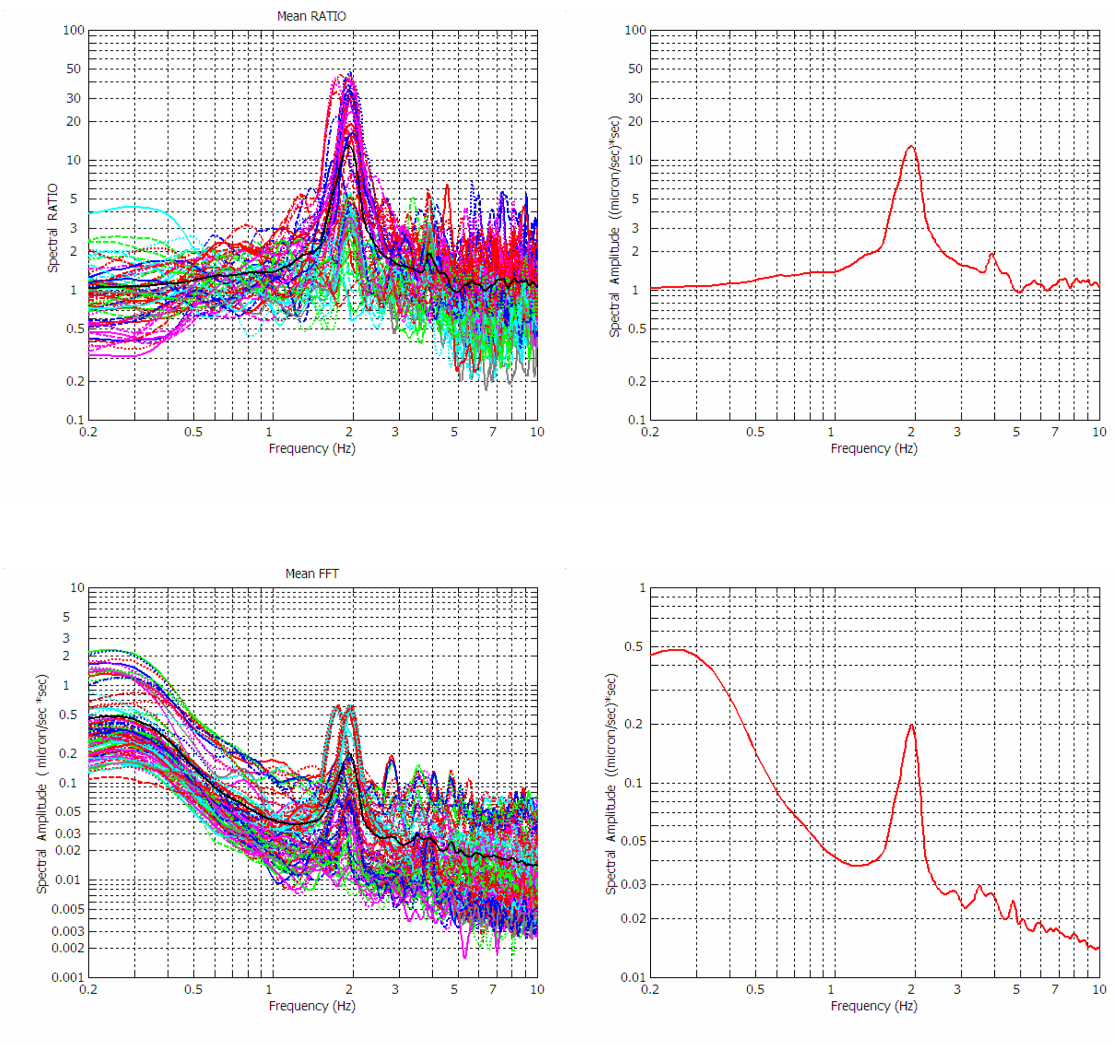

Figure 3.2: Spectral amplitude and spectral ratio for site 1.

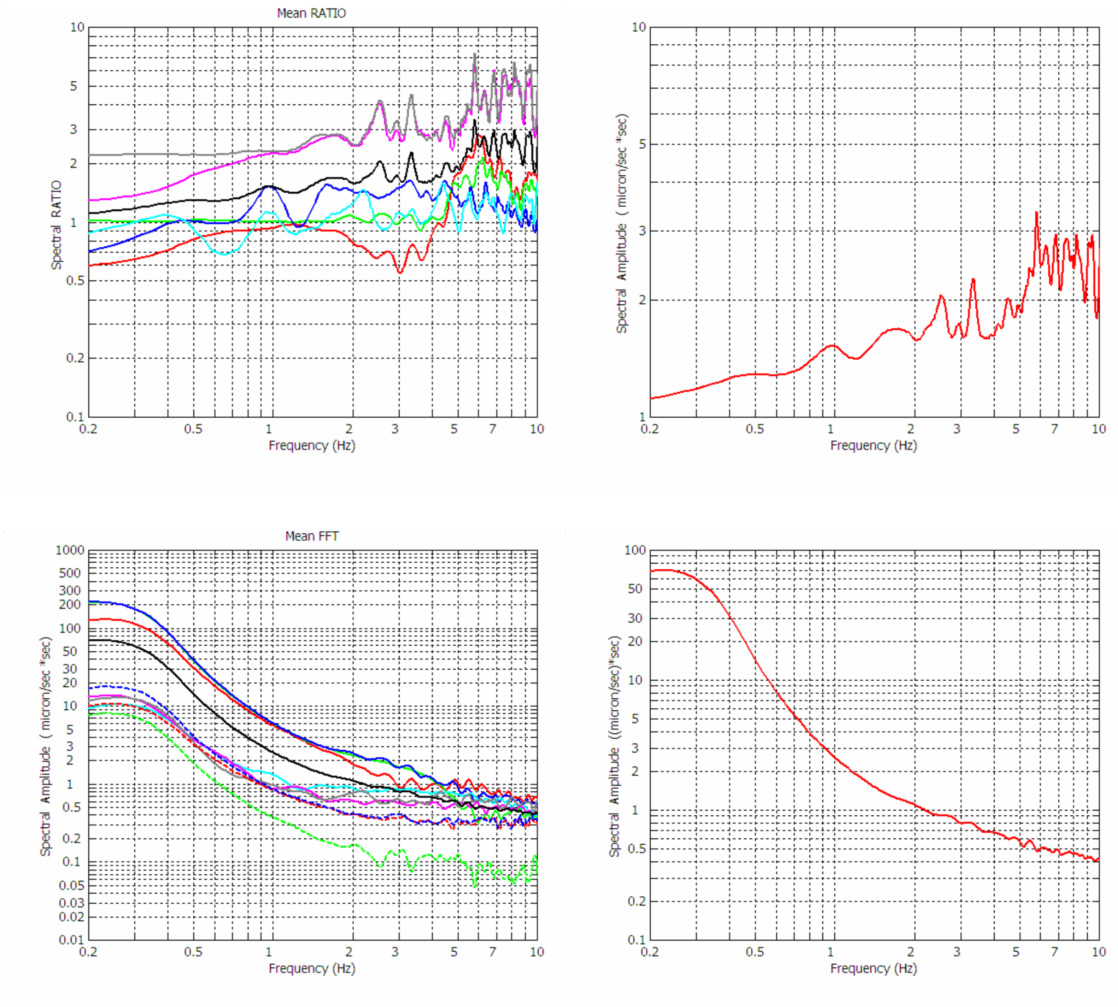

Figure 3.3: Spectral amplitude and spectral ratio for site 2.

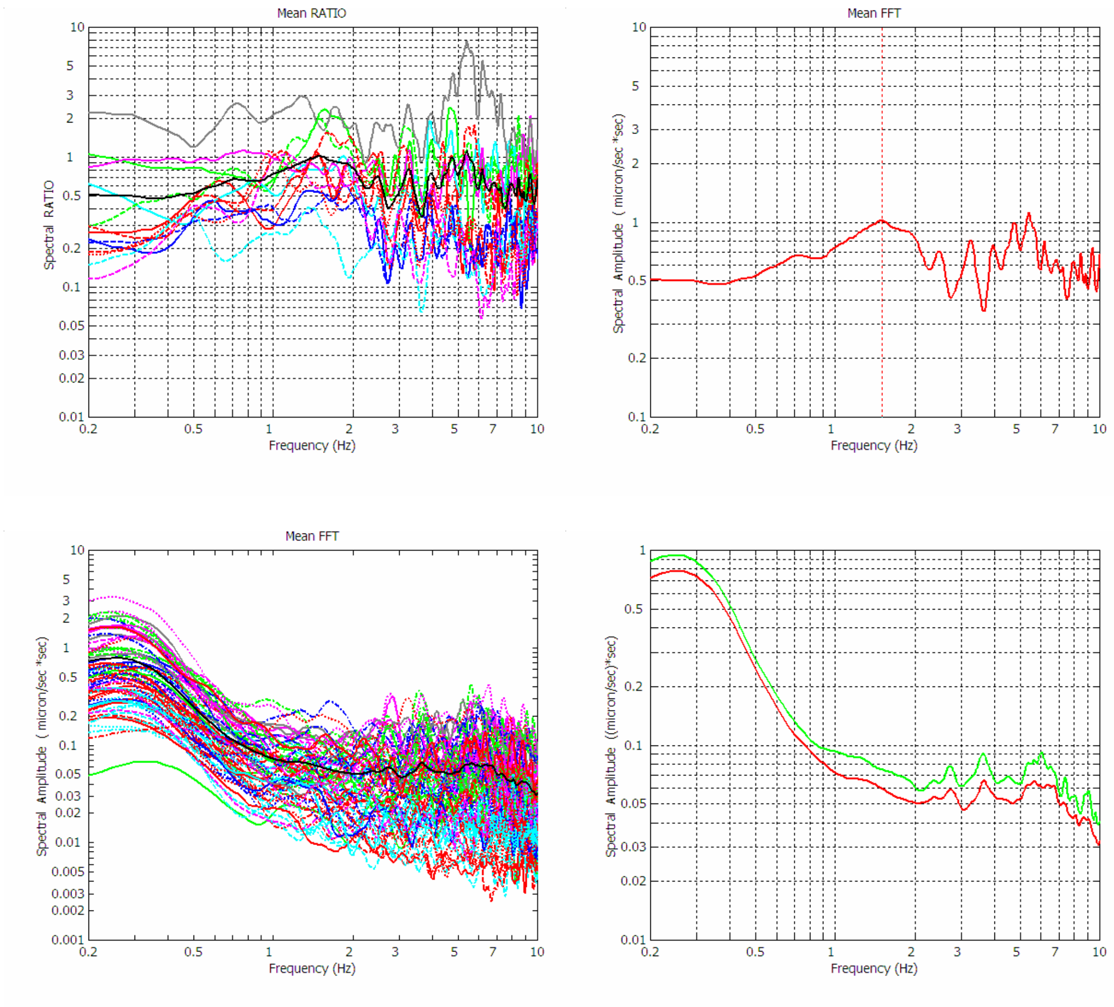

Figure 3.4: Spectral amplitude and spectral ratio for site 3.

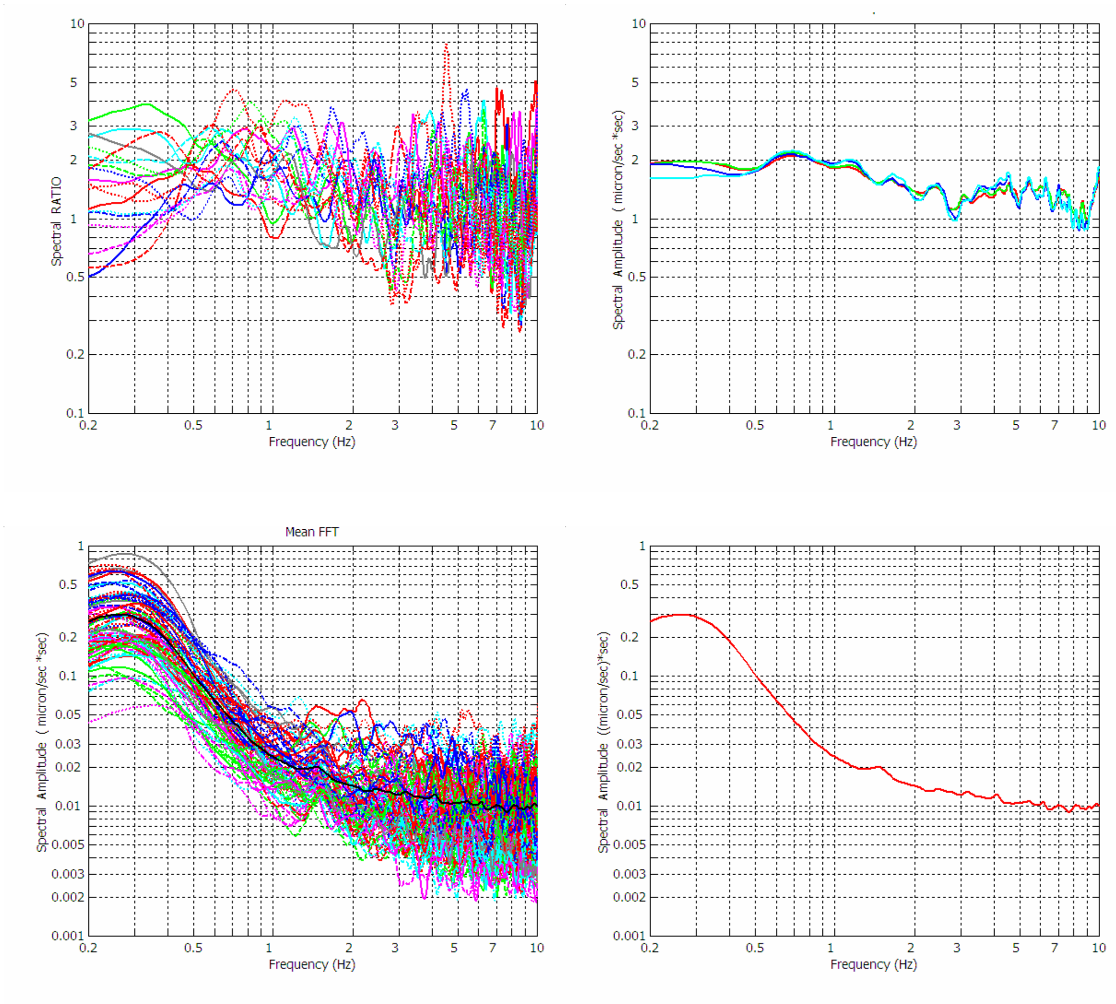

Figure 3.5: Spectral amplitude and spectral ratio for site 4.

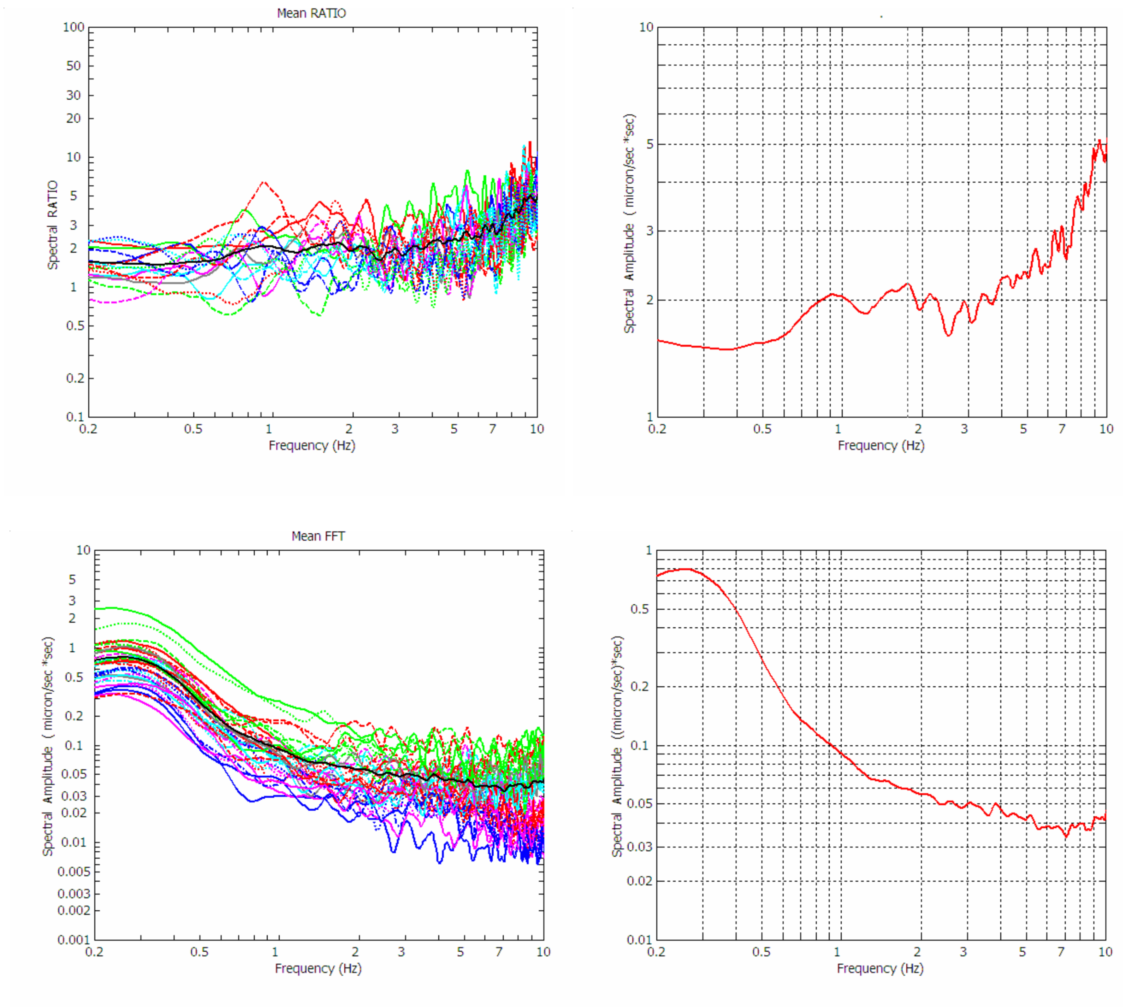

Figure 3.6: Spectral amplitude and spectral ratio for site 5.

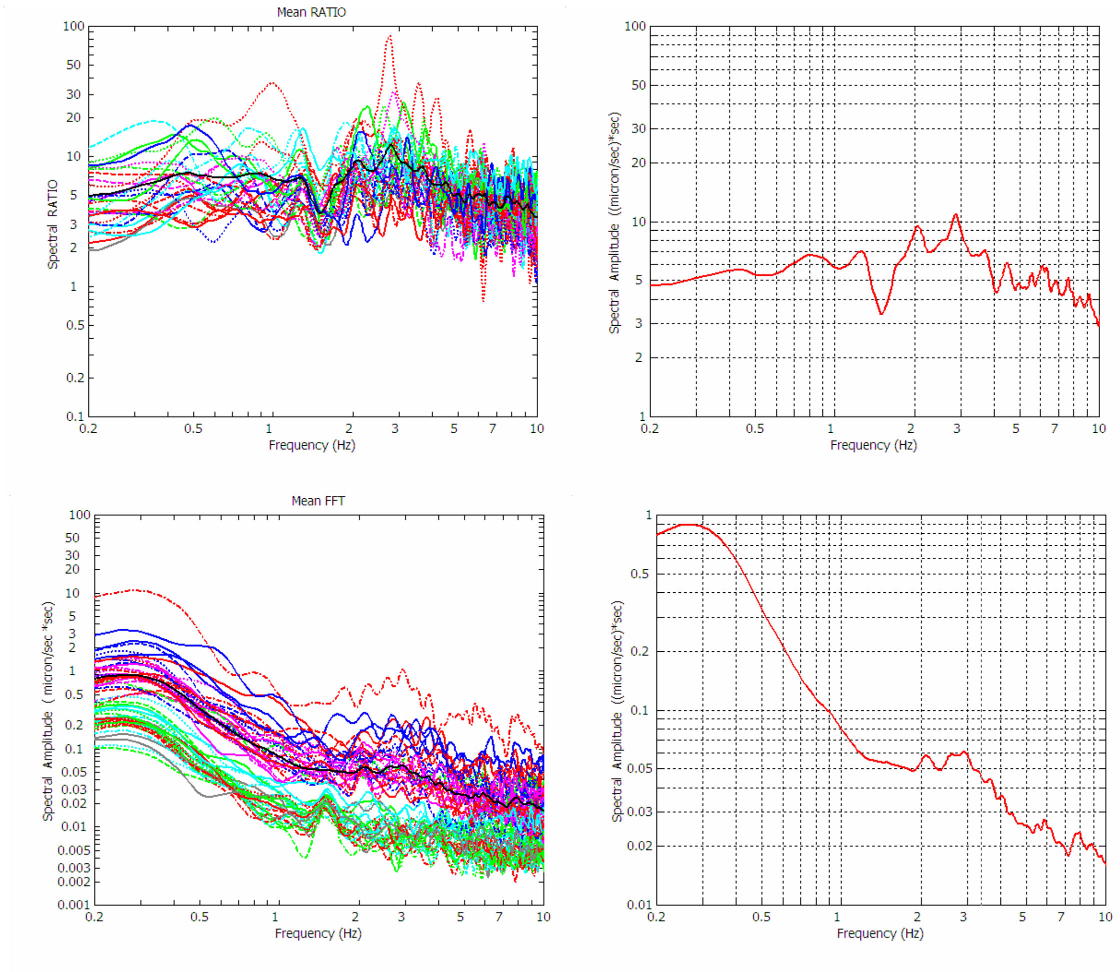

Figure 3.7: Spectral amplitude and spectral ratio for site 6.

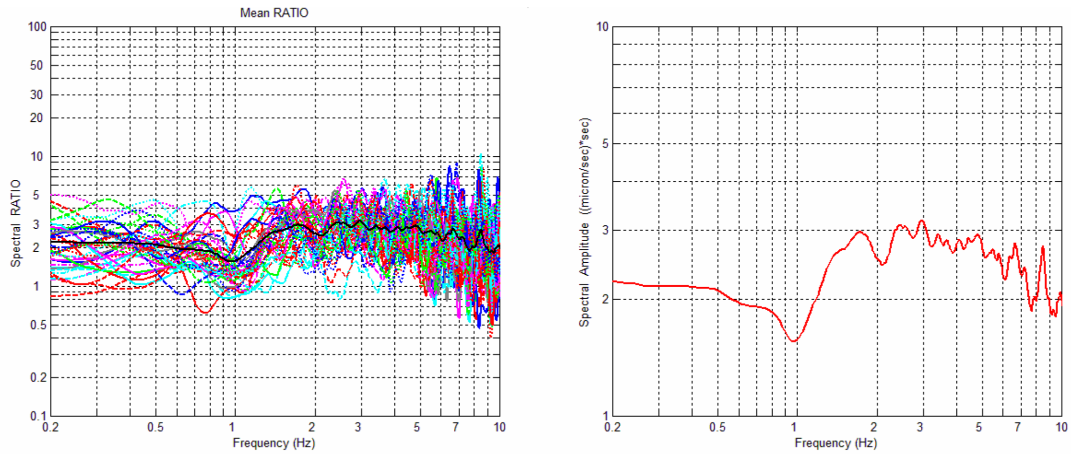

Figure 3.8: Spectral ratio for site 7.

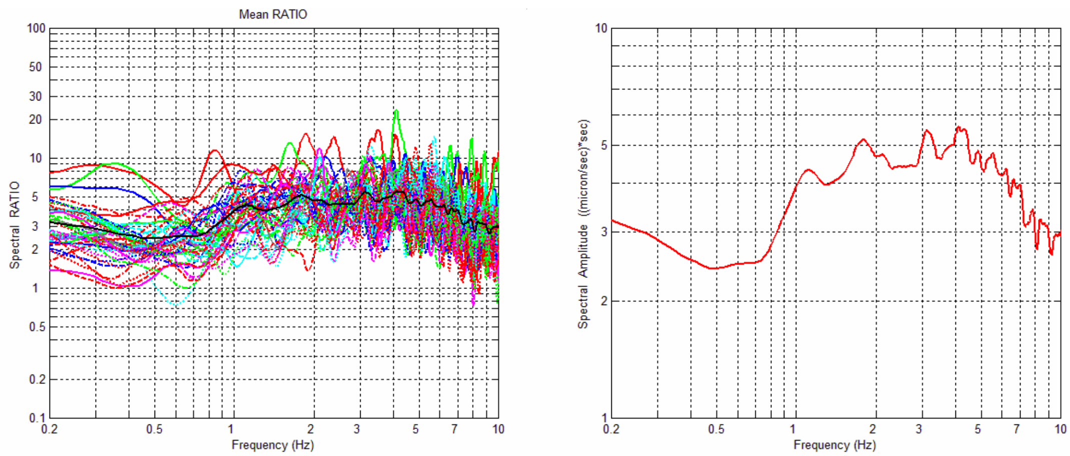

Figure 3.9: Spectral ratio for site 8.

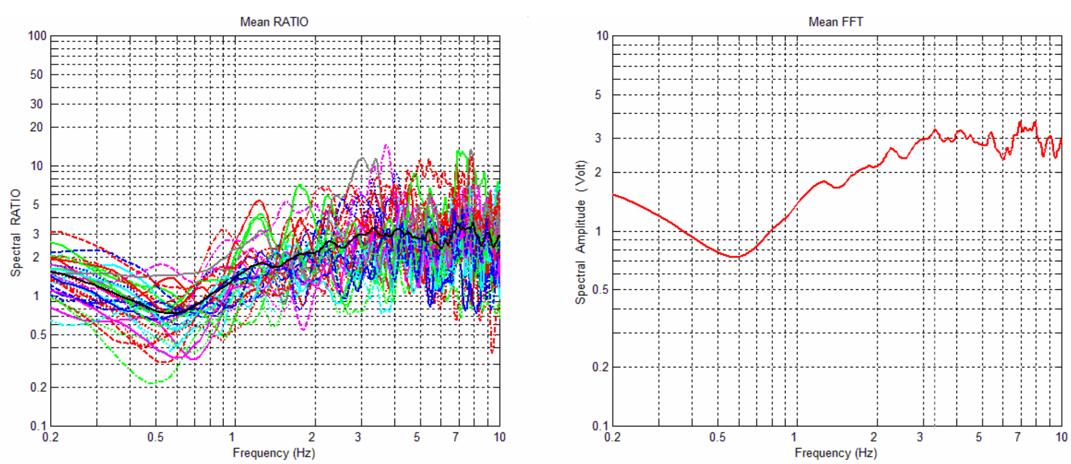

Figure 3.10: Spectral ratio for site 9.

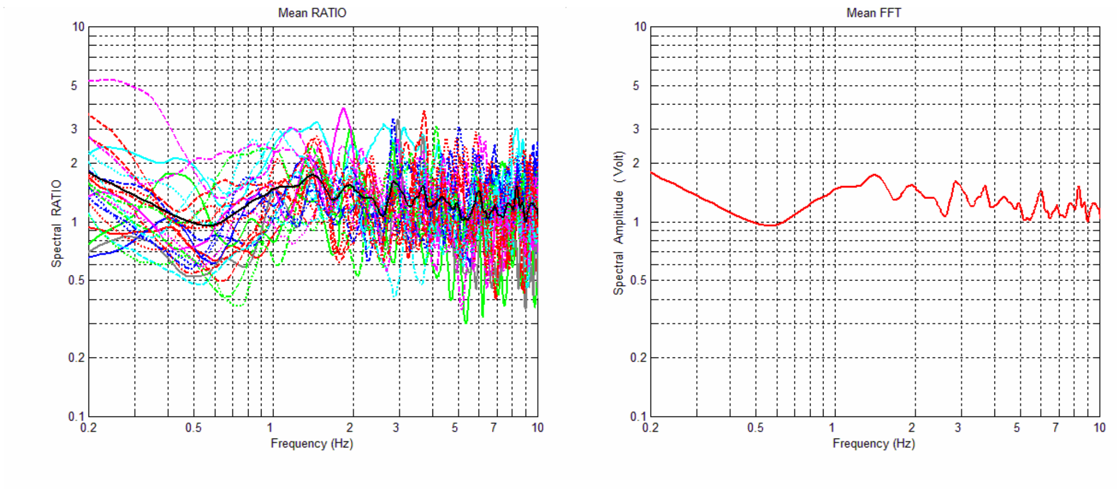

Figure 3.11: Spectral ratio for site 10.

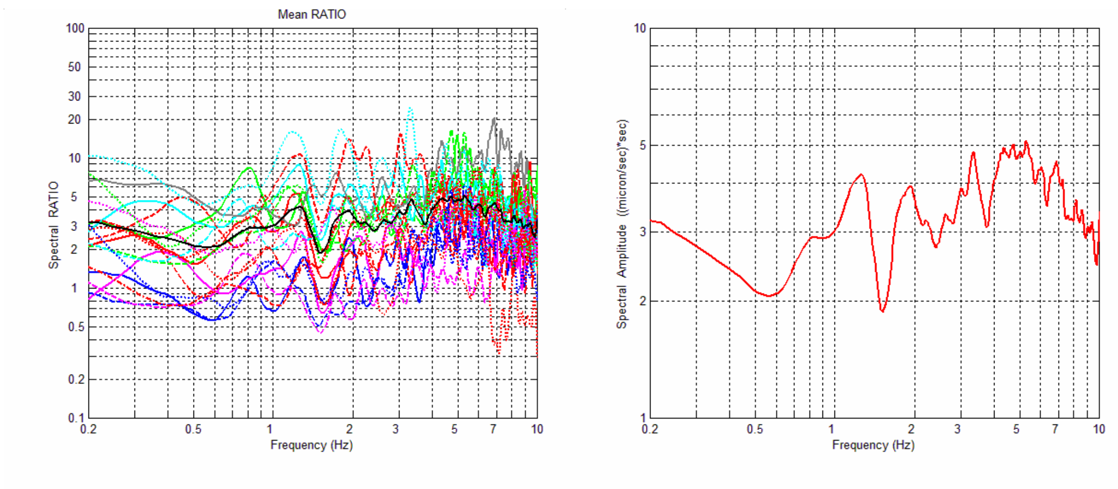

Figure 3.12: **Spectral ratio for site 11.**

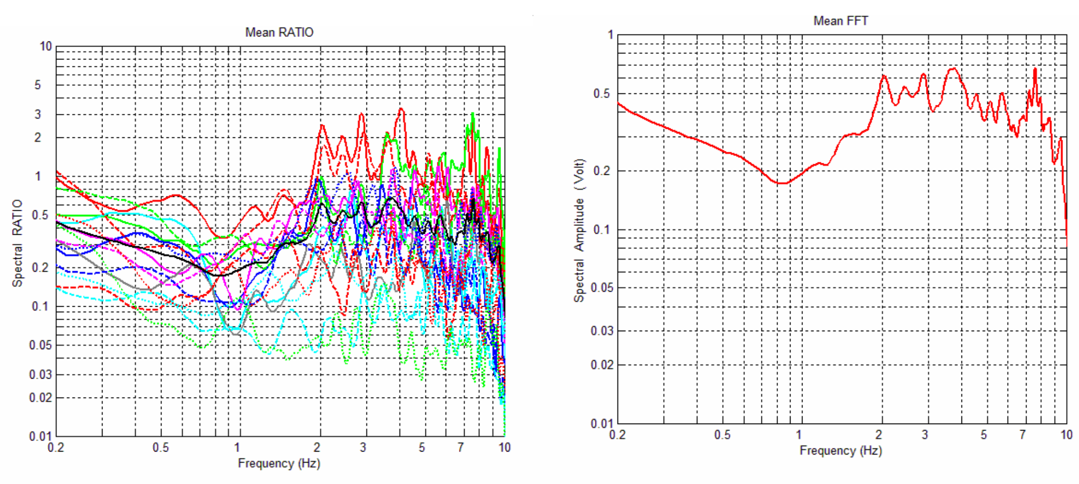

Figure 3.13: Spectral ratio for site 12.

Table 1. The results show obvious differences among the dominant frequencies even when the studied area is small.

The distribution of the dominant frequency values of the measured sites varied from the southern part to the northern part as well as from the upper part to the lower part of Rawabi city (Stage 1 – phase 1). Quite large differences in amplification between and around 1 and 12 were computed for measured sites (see table 3.1, sites 1-12). According to geotechnical and geophysical investigations, the city center area in Rawabi city is lying on mountains and consists of unconsolidated carbonates (see table 3.1 and the locations of measured sites 1-12 presented in Fig. 3.1). Where the thickness of marly formations varies between 10 -20 m, amplifications between 2 and 12 for dominant natural period range of 0.4 – 1 sec were obtained. In the

TABLE 3.1: Results list of dominant frequencies, amplifications and natural periods.

Microtremor Measurements				Building Codes*
Site	**Dominant Frequency Hz**	**Amplification Factor**	**Natural period sec** (Ts)	**Natural period Sec** (T_b)
1	2	11-12	0.5	1.5
2	2.2	2-3	0.45	1.5
3	1.5 – 2	2	0.5 – 0.66	0.55 (0.455)
4	0.5 – 1	2 – 3	1- 2	0.55 (0.455)
5	2 – 1	2.5	0.5 – 1	0.55 (0.455)
6	0.8 – 2	7 – 9	0.5 – 1.25	0.55 (0.455)
7	1.8 – 2	3	0.5 – 0.55	1.5
8	1 – 2	4 - 5	0.5 – 1	1.5
9	1.5 – 2	4 - 5	0.5 – 0.66	1.5
10	1 – 2	2.5 - 3	0.5 – 1	0.55 (0.455)
11	1 – 2	4 - 8	0.5 – 1	1.5
12	2	1 - 2	0.5	0.55 (0.455)

***** *According to Uniform Building Code (UBC97)*, *International Building Code (IBC) and Jordanian Building Code (JBC).*
Att. the values between two brackets according to JBC

other part of the investigated area (sites 3, 4, 5, 10, and 12), which is located on limestone rocks covered with a thin layer of soil (see Table 3.1, and Fig. 3.1), the amplification was relatively low and it varied between 1 and 3.

3.3 The Fundamental Natural Period of Proposed Buildings in Rawabi City (staqge 1 – phase 1)

The fundamental period of proposed buildings in Rawabi city (buildings which will be built in stage 1 – phase 1) were calculated using the Uniform Building Code (UBC 97), International building Code (IBC) and Jordanian Building Code (JBC), see Table (3.1). All the proposed buildings in the city center area have fundamental periods (T_b) more than the characteristic site period (Ts). This means that the double resonance[1] phenomena will be avoided in this area. Reducing the marly stratum level in the city center area by 10 – 20 meters as proposed in the master plan will result in reducing the amplification factor mentioned above (see amplification factor for sites 1, 2, 6, 7, 8, 9 and 11 in table 3.1) and in some cases the amplification factor expected to be less than 2, which is considered to be relatively safe. In other words, the city center site resonance will be avoided. For the other areas (Hai 1 – 6), the amplification factor is relatively small.

3.4 Conclusions

The characteristic site period (or site dominant frequency $\mathbf{T_s}$) which depends on the thickness (H) and shear wave velocity (V_s) of the soil provides a very useful indication of the period of vibration at which the most significant amplification can be expected. The site dominant natural period varies between 0.8 - 1.25 sec at the city center area and between 0.5 – 1 sec at the other areas.

Based on the effects of local geology, there is a strong correlation between the different values of the amplification factor and the changes in the lithology. Where most of the areas at Hai, 1, 2, 3, 4, 5 and 6, consist of consolidated carbonates bedrock, slight amplification is expected in comparison with the quite larger amplification factors computed at the city center areas that consist of non-consolidated carbonates bedrock (marly materials).

[1] Amplification of bedrock motion by the soil deposit and amplification of the soil motion by the structure.

Regarding the spectral ratio analyses of the selected sites in the study area, the high spectral ratio range of 4-12 is shown in the sites 1, 2, 6, 7, 8, 9 and 11 in the frequency range of about 0.8 - 2 Hz.

Reducing the marly stratum level in the city center area by 10 – 20 meters as proposed in the master plan, will result in reducing the amplification factor mentioned above (see amplification factor for sites 1, 2, 6, 7, 8, 9 and 11 in table 3.1) and in some cases the amplification factor expected to be less than 2, which is considered relatively safe. In other words, the city center site resonance will be avoided. For the other areas (Hai 1 – 6), the amplification factor is relatively small.

For more details about the dominant frequency or dominant natural period, see the microzonation map shown in appendix no. 5